Surface modification of silica-based marine sponge bioceramics induce hydroxyapatite formation

Alexandre A. Barros[1,2], Ivo M. Aroso[1,2], Tiago H. Silva[1,2], João F. Mano[1,2], Ana Rita C. Duarte[1,2*] and Rui L. Reis[1,2]

[1] 3B's Research Group – Biomaterials, Biodegradables and Biomimetics, University of Minho, Headquarters of the European Institute of Excellence on Tissue Engineering and Regenerative Medicine, AvePark, 4806-909 Taipas, Guimarães, Portugal

[2] ICVS/3B's – PT Government Associate Laboratory, Braga/Guimarães, Portugal

* Corresponding author. Address: 3B's Research Group – Biomaterials, Biodegradables and Biomimetics, University of Minho, Headquarters of the European Institute of Excellence on Tissue Engineering and Regenerative Medicine, AvePark, 4806-909 Taipas, Guimarães, Portugal

E-mail: aduarte@dep.uminho.pt

ABSTRACT

Marine biomaterials are a new emerging area of research with significant applications. Recently, researchers are dedicating considerable attention to marine-sponge biomaterials for various applications. We have focused on the potential of biosilica from *Petrosia ficidormis* for novel biomedical/industrial applications. A bioceramic structure from this sponge was obtained after calcination at 750ºC for 6 hours in a furnace. The morphological characteristics of the 3D architecture were evaluated by scanning electron microscopy (SEM) and micro-computed tomography revealing a highly porous and interconnected structure. The skeleton of *Petrosia ficidormis* is a siliceous matrix composed of SiO_2, which does not present inherent bioactivity. Induction of bioactivity was attained by subjecting the bioceramics structure to an alkaline treatment (KOH 2M) and acidic treatment (HCl 2M) for 1 and 3 hours. *In vitro* bioactivity of the bioceramics structure was evaluated in simulated body fluid (SBF), after 7 and 14 days. Observation of the structures by SEM, coupled with spectroscopic elemental analysis (EDS), has shown that the surface morphology presented a calcium-phosphate CaP coating, similar to hydroxyapatite (HA). The determination of the Ca/P ratio, together with the evaluation of the characteristic peaks of HA by infra-red spectroscopy and X-ray diffraction, have proven the existence of HA. *In vitro* biological performance of the structures was evaluated using an osteoblast cell line andthe acidic treatment has shown to be the most effective treatment. Cells were seeded on the bioceramics structures and their morphology, viability and growth was evaluated by SEM, MTS assay and DNA quantification, respectively, demonstrating that cells are able to grow and colonize the bioceramic structures.

Keywords: Marine Sponge, bioactivity, Biosilica, scaffold; tissue engineering.

1. INTRODUCTION

The study of marine natural products continues to expand with a steady increase in the annual number of new compounds described and also with the number of registered patents[1-3]. Last decade, comprehensive reviews have systematically pointed to sponges (*Porifera*) as the most promising for blue biotechnology, as they constantly rank first for the number of derived novel metabolites with pharmaceutical potential (e.g., anticancer, antiviral, anti-inflammatory) [2, 3].

The leading role of *Porifera* within blue biotechnology stems from their long evolutionary history and extreme plasticity. Sponges are the oldest phylum in the animal kingdom dating back to over 600 million years [4], and one of the most versatile on earth. With over 8000 existing species distributed across all aquatic environments, sponges have been able to specialize and adapt to an extraordinarily variety of habitats (from tropical coral reefs to polar waters, from freshwater to the ocean deepest floors, up to the intertidal and into transition habitats), dominating many of them in terms of abundance and biomass [4].

Sponges are soft bodied composed by organic and inorganic compounds that filter the water for food, and harbor yet undescribed associated microorganisms. It is no wonder that they have developed an incredibly diverse chemical arsenal to deter predators, compete for space, reject fouling organisms, and fight pathogens[5]. The biodiversity that characterizes the marine environment represents an enormous potential for the study of novel microstructures.

The use of biostructures derived from the marine environment for application as biomaterials is very recent [6]. For instance, several authors have proposed, in the last years, the use of different marine species like coral skeletons, sea urchins and sponges as three dimensional biomatrices[7-11]. The results have confirmed that the three dimensional topography and the surface parameters of these materials influence positively cell differentiation. Furthermore, topography and composition of the material have been proven to affect cellular functions, such as adhesion, growth, motility, secretion and apoptosis[12, 13]. The particular interest in *Porifera* sponges is related to the fact that these are the only animal organisms able to polymerize silica to generate massive skeletal elements (spicules) [14], in *Demospongiae* class. The spicules can constitute up to 75% of the dry weight of the organism and the mineral skeleton of these sponges is composed of amorphous silica $(SiO_2)_2$-$5.H_2O$ and may contain traces of other elements such as

S, Al, K and Ca [15]. Sponges have also been noted to produce many unique biosilica structures that provide a magnificent source of inspiration for novel products in various fields following a biomimetic approach. The present state-of-the-art in the field of sponge biosilica has been summarized in different review articles [16] and books [17, 18].

In particular, in this work we focus on the potential for novel biomedical applications of biosilica from *Petrosia ficidormis*, hereby taking advantage of the unique 3D bioceramics structure that can act as scaffold for tissue engineering applications.

2. EXPERIMENTAL SECTION

2.1 Materials.

Sponge samples

Petrosia ficidormis (PET) sponges were collected in Mediterranean Sea in the Spanish east coast, and were kindly provided by Ronald Osinga (Porifarma). The samples were frozen after collection. Prior to any experiment the sponges were salt leached and freeze dried.

Chemicals

All chemical reagents were ACS reagent grade and were used as received.

2.2 Modification of Sponges

The bioceramic structure from the sponge was obtained after calcination at 750ºC for 6 hours in a furnace. The biosilica structure obtained was modified to induce bioactivity by subjecting the bioceramics structure to two different surface treatments. An alkaline treatment with potassium hydroxide (KOH) 2M at reflux temperature and acidic treatment with hydrochloric acid (HCl) 2M at room temperature for 1h and 3h under stirring were performed. After the surface modification reaction, the sample was washed with distilled water for several times and dried overnight in a vacuum oven at 37ºC. The procedures tested were performed under conditions such that the original structural properties would be preserved but at the same time promoting the creation of hydroxyl groups on the surface of the 3D architecture.

2.3 Bioactivity tests

The alkaline and acid surface treated 3D bioceramics from PET (three replicas per time point) were immersed in simulated body fluid (SBF) at a ratio of 1:10 (bioceramics mass, in g: SBF volume, in mL) for 7 and 14 days and were maintained in a thermostat water bath at 37ºC and 60

rpm. At each time point the bioceramic structures were recovered, washed with distillated water and dried at 37ºC.

2.4 Characterization

The bioceramic structures (modified and unmodified) were studied by different physico-chemical characterization techniques, after calcination and after the bioactivity tests.

2.4.1 Scanning Electron Microscopy

Scanning electron microscopy (SEM) was used to analyze the surface morphology and to evaluate the formation of CaP crystals. All the samples were sputter-coated with gold before analysis. Micrographs were acquired on a Leica Cambridge S360 microscope (Leica Cambridge, United Kingdom) using beam energy of 15.0kV and a working distance (WD) of 19 mm.

2.4.2 Energy Dispersive X-ray Spectroscopy.

Energy dispersive X-ray spectroscopy (EDS) was used to characterize the nature and relative quantity of the chemical elements present on the surface of the bioceramics. The analysis was performed using a Link eXL-II spectroscope (Oxford Instruments, United Kingdom), at an energy of 15.0 keV, coupled to SEM. All the samples were carbon coated before the analysis.

2.4.3 Micro-computed tomography

Micro-computed tomography (μ-CT) was used to evaluate the porosity and pore size of the 3D bioceramic structures. The images were acquired on a high-resolution micro-CT SkyScan 1072 scanner (Skyscan, Belgium) using a voltage of 189 kV and a current of 46 μA. After image acquisition the noise was reduced with nRecon software. CT Analyser® software (SkyScan, Belgium) was used to obtain representative data sets of the samples and converting them into 2D images.

2.4.4 Compressive mechanical analysis

Compressive mechanical analysis of the 3D bioceramic structures were measured using an INSTRON 5540 (Instron Int. Ltd., High Wycombe, UK) universal testing machine with a load cell of 1 kN. The compression tests were carried out at a crosshead of 2 mm min^{-1}, until the structure fracture. The compressive modulus was calculated from the initial linear slope on the stress/strain curves.

2.4.5 Fourier transform infrared spectroscopy

The infrared spectra of the bioceramic samples, before and after immersion in SBF, were obtained on an IR Prestige-21 spectrometer (Shimadzu, Japan), using 32 scans, a resolution of 4 cm^{-1} and a wavenumber range between 4400-400 cm^{-1}.The samples were powdered, mixed with potassium bromide, and the mixture was molded into a transparent pellet using a press (Pike, USA).

2.4.6 X-ray Powder Diffraction

X-ray diffraction (XRD) was used to identify the crystallographic planes of the CaP crystals deposited on the surface of bioceramics, after immersion in SBF solution. Diffraction patterns were collected on a Bruker D8 Discover, operating with Cu-Kα radiation, in the θ/2θ mode, between 6º and 70º, with a step increment of 0.04º and an acquisition time of 1 s per step.

3 Cytotoxicity and cell adhesion studies

3.1 Cell culture

A human osteogenic sarcoma cell line (SaOS-2 cell line, European Collection of Cell Cultures, UK), was maintained in basal culture medium DMEM (Dulbecco's modified Eagle's medium; Sigma– Aldrich, Germany), plus 10% FBS (heat-inactivated fetal bovine serum,

Biochrom AG, Germany) and 1% A/B (antibiotic–antimycotic solution, Gibco, UK). Cells were cultured in a humidified incubator at 37ºC in a 5% CO_2 atmosphere.

3.2 Direct contact studies

Confluent SaOS-2 cells were harvested and seeded in the samples as follows. Samples were distributed in a 48-well cell culture plate (BD Biosciences, USA). Samples were initially immersed in sterile PBS. After, PBS was removed and a drop (20µl) of a cell suspension with a concentration of 5 x 10^5 cells/ml was added to each material. The cells-samples constructs were statically cultured for 1, 3, 7 and 14 days under the culture conditions previously described.

3.2.1 MTS Assay

Cell adhesion to the surface of the materials was determined after the pre-determined culture times by the MTS assay. The cell-scaffold were transferred to a new culture plate in order to evaluate the presence of viable cells only on the different materials. Cell metabolic activity at each culture time was determined using the Cell Titer 96Aqueous One Solution Cell Proliferation Assay (Promega, USA) according to the instructions of the manufacturer. Absorbance was measured at 490 nm using a microplate reader (Synergie HT, Bio-Tek, USA). Optical density was determined for each time point and compared to polystyrene tissue culture plate, used as a positive control. All cytotoxicity screening tests were performed using three replicates.

3.2.2 DNA Quantification

After each time point, cells were lysed by osmotic and thermal shock and the obtained supernatant was used for DNA quantification. Cell proliferation was evaluated by quantifying the DNA content along the time of culture using the PicoGreen dsDNA kit (Molecular Probes, USA) according to the instructions of the manufacturer. Fluorescence was read (485 nm/528 nm of excitation/emission) in a microplate reader (Synergie HT, BioTek, USA), and the DNA amount calculated from a standard curve.

3.2.3 Alkaline phosphatase (ALP) activity Assay

The analysis of ALP activity was performed after cell lysis, based on the conversion of p-nitrophenyl phosphate (Sigma,Germany) into p-nitrophenol. In each assay 20 µL of lysate were incubated with 80 µL of p-nitrophenyl phosphate solution (0.2% w/w, in diethanolamine, Sigma, USA) in a transparent 96 well microplate, at 37ºC, for 45 minutes. The reaction was stopped using 80 µL of a 2M NaOH (Sigma, USA) and 0.4 mM EDTA (Sigma, USA) solution. Optical density was read at 405 nm using a microplate reader (Synergie HT, Bio-Tek, USA). A calibration curve was previously prepared using p-nitrophenol standard solutions (Sigma, USA) and used to extrapolate the ALP activity values. These values were then normalized against dsDNA results obtained within the same experiments.

4 Statistical analysis

Statistical analysis of the data was performed using GraphPad Prism version 5. Normality was verified by the Shapiro-Wilk test. Normal distributed data were then analysed using one-way ANOVA with Bonferroni's post-test; when normality was not observed the non-parametric Kruskall-Wallis test was performed. Differences between the groups with $p<0.05$ were considered to be statistically significant.

5. RESULTS

Images of the raw material of *Petrosia ficidormis* (PET) and the 3D bioceramic structure are presented in **Figure 1.** Optical micrographes, SEM images and the 3D reconstruction of the sponges by Micro-CT analysis are also shown.

5.1 Structural Analysis

The EDS analysis showed that the 3D bioceramic structure is composed of silicon and oxygen atoms in a SiO_2 stoichiometric proportion. **Additionally, we can observe that after the calcination process, all the organic components are removed, as denoted by the absence of carbon, along with other constitution elements (Na, P, S, Cl, K and Mg) of the organic**

materials leaving only the inorganic structure; the data supported the absence of carbon element in the EDS results (**Figure 1**).

[FIGURE 1]

Micro-CT analysis, before and after calcination, showed an increase of the porosity in 3D bioceramic structures. The raw material presented a porosity of 73%, and after calcination this value increased to 83%. The same trend was found for the mean pore size which increased from 364 μm to 510 μm.

The mechanical performance of the 3D bioceramic structure under compression loading was acessed in dry and in wet state and the results are presented in **Table 1**.

Table 1. *Compressive modulus of raw material and 3D bioceramic structure in dry and wet state.*

Sample		***Compressive Modulus (MPa)***
Raw Material	***Dry***	*3.21 (±1.74)*
	Wet	*1.03 (±0.16)*
3D Bioceramics	***Dry***	*3.34 (±1.14)*
	Wet	*1.12 (±0.57)*

5.2 Surface modification

Surface modifications have been proposed to enhance or induce bioactivity properties in biomaterials[19]. The two treatments were chosen based on different results published in the literature. It has been previously reported that the alkaline treatment of silicon surfaces at pH higher than 13 can result in the formation of hydroxyl groups [20]. Likewise, under acidic media,

glass surfaces can be modified to produce a superficial layer of Si-OH groups[21]. A schematic representation of the surface modification process is presented in **Figure 2**.

[FIGURE 2]

After the surface modification procedures, samples were observed by SEM (**Figure 3)**. It was observed that the 3D structure was maintained after the treatments with an apparent increase of the surface roughness, compared to the control structures.

[FIGURE 3]

5.3 In vitro evaluation of bioactivity of the 3D bioceramics after chemical treatment

The *in vitro* bioactivity assessment was carried out by immersing the 3D bioceramics in simulated body fluid, which contains ions and minerals at a concentration similar to the human plasma [22]. When evaluating the results of the bioactivity for 1 and 3 hours of treatment, both for alkaline and acidic treatments, no differences were observed. Therefore, only the results for 1 hour reaction will be presented here.

The pH of SBF solution was observed to be constant within the time period studied: 7.85 ±0.7 in the case of KOH treated samples a 6.98 ± 1.2 in the case of HCl treated samples. The SEM micrographs of the surface of the 3D biomatrices after immersion in SBF for different time points are presented in **Figure 4**.

[FIGURE 4]

Chemical analysis performed by EDS provided information for the determination of the Ca/P ratio of the crystals present. The determined Ca/P ratios are presented in **Table 2.**

Table 2. *Ca/P atomic ratio calculated from the EDS data, for the modified and unmodified 3D bioceramics structures, after immersion in SBF for different times.*

	CTR	KOH	HCl
7 Days	0	1.50	1.69
14 Days	0	1.62	1.67

The stoichiometry of HA refers to the exact atomic ratio of Ca/P (10/6 or 1.67) in this ceramic. Deviation from the exact Ca/P ratio destabilizes the crystal and enhances the dissolution of the material. Thus, calcium deficient HA with a Ca/P ratio of 1.60 is slightly more bioactive than stoichiometric HA with a Ca/P ratio of 1.67 [23, 24].

FTIR and XRD analysis were performed to better describe the new crystals on the surface of the 3D bioceramic structures. FTIR spectroscopy allowed the identification of most of Ca/P vibrational modes present in apatites. The analysis confirms the presence of characteristics peaks of carbonates (n3 1400 - 1550 cm^{-1}; n4 650 - 750 cm^{-1}) and phosphates (n3 1000 -1150 cm^{-1}; n4 500 - 620 cm^{-1}), from hydroxyapatite. XRD patterns (**Figure 5**) of the 3D bioceramic surfaces treated from PET, confirmed the presence of the crystallographic diffraction planes of: hydroxyapatite - (2 1 0 hkl, 31.820 2Θ (λ_{CU} = 1.5406 Å), (2 1 1 hkl, 328.967 2Θ (λ_{CU} = 1.5406 Å); calcium oxide - 2 0 0 hkl, 37.361 2Θ (λ_{CU} = 1.5406 Å); and some intermediate crystals (DCPD-Brushite (1 2 1 hkl, 20.935 2Θ (λ_{CU} = 1.5406 Å)).

[FIGURE 5]

5.4 In vitro biological studies

SaOS-2 cell line was chosen to perform the in vitro biological assessment as it is an osteoblastic-like cell line. The choice of this cell line regards the final application envisaged which would be bone regeneration. The cytotoxicity effects and the cell viability for a certain culture time, on the 3D bioceramic structures, treated with KOH and HCl were evaluated by MTS assay (**Figure 6**).

In what concerns the metabolic activity of SaOS-2 cells, when cultured with the materials, lower values than for the control were obtained in case of PET and KOH. For HCl treated samples the values, in general, were found to be higher than the control. These results

demonstrated that HCl treated samples present a better performance for cells, nevertheless, none of the samples present cytotoxic effect.

[FIGURE 6]

The cell proliferation was evaluated by quantifying the DNA content along the time of culture. In **Figure 7** the double stranded DNA (dsDNA) content of SaOS-2 Cells cultured for 1, 3, 7 and 14 days on 3D bioceramic structures with KOH and HCl treatments (1hour reaction) is presented.

[FIGURE 7]

Alkaline phosphatase is an important enzyme in hard tissue formation, highly expressed by mineralized tissue cells. The analysis of ALP activity was performed and the results are presented in **Figure 9**. Alkaline phosphatase activity in the cells adhered on the surface of the KOH treated samples was lower than in the cells adhered to the material without chemical treatment (PET). However, a different result was obtained for the HCl treated samples that present higher values of alkaline phosphatase expression after 7 and 14 days.

The presence and adhesion of cells in 3D bioceramics ceramics with and without treatments after 7 and 14 days in culture were observed by SEM analysis. **Figure 9** shows the presence and adhesion of the osteoblastic cell line after 7 and 14 days in our 3D bioceramics structure regardless of sample. Moreover, the images suggest that HCl treated samples present higher adhesion, both for 7 days and for 14 days.

[FIGURE 8]

[FIGURE 9]

6. DISCUSSION

In this work we hypothesized that three-dimensional (3D) bioactive bioceramics structures can be obtained from marine-sponges. The use of 3D structures from marine origin for biomedical applications has been proposed in the last years by different authors [8]. Examples are the use of different marine species like coral skeletons, sea urchins and sponges as three dimensional biomatrices [25]. Taking into account the variety in siliceous-nature of the chemical compositions, we also hypothesize that sponges may constitute an adequate source of 3D bioceramic scaffolds to be used in tissue engineering and regenerative medicine (TERM). In a previous work, the structure of PET, after calcination, demonstrated to be an interesting structure to act as scaffold in tissue engineering, particularly for bone tissue regeneration, but the bioactivity test revealed an inert surface [7].

The inorganic structure from the marine sponge PET was obtained after calcination. The structure presents a stable 3D architecture which, in a biomimetic perspective, can inspire the development of scaffolds for bone TERM applications.

Morphological characteristics such as porosity, mean pore size and interconnectivity are determining factors that define the applicability of a matrix as a TE construct. Generally, a surface with high porosity favors cellular growth, as a greater area is available for osteoblast adhesion and migration[26]; this, in turn, facilitates the proliferation of the cells. Furthermore, the bonding between the bone and the substitute material is more likely to take place on a porous surface. In 3D structures such as bone scaffolds, the dimension of the pores and their interconnectivity play also an importante role [27]. With well-interconnected pores, cells can easily reach all parts of the material, leading to a more complete osteointegration [28]. The morphological properties suggest the suitability to act as scaffold in tissue engineering approaches. *Cunninggam, E. et al* [8], in a similar study with a diferente marine sponge (*Spongia agaricina*) obtained identical results in terms of porosity, mean pore size and interconnectivity.

The values of compressive modulus before and after calcination indicate that this procedure did not affect the mechanical behaviour of 3D structure. However, a pronounced decrease of the compressive modulus (from ~3MPa to ~1MPa) is observed in the wet state.

Overall, the mechanical performances achieved in dry and wet sates are in the range of the mechanical properties of human bone [29], particularly in low-bearing load bone areas.

Using bioactive scaffolds as a bone substitute is the most obvious choice for TERM applications, as these can replicate the mineral composition and the behavior of human bone. Bioactive materials are preferred, where bioactivity is defined as the ability of the material to induce the formation of an interfacial bonding between the implant and living tissues, without the formation of a fibrous capsule separating the biomaterial and the tissue[30, 31]. Hydroxyapatite (HA), $Ca_{10}(PO_4)_6(OH)_2$, is a chemical compound widely employed as a biomaterial, more specifically as a bone substitute. It is highly biocompatible and osteoconductive; in fact, it promotes the formation of new bone by favoring the growth of osteoblast cells [32]. Mineral scaffold biocompatibility and its effectiveness as a bone substitute material depend, however, on several factors; the ratio between calcium and phosphorous is particularly important.

Marine-sponges have not been yet fully explored for their ceramics or as a bioactive 3D bioceramic structure as opposed to other marine sources[8, 10, 33-35]. Although the morphological and mechanical features of the PET structure are very interesting, preliminary results on the bioactivity of the sponge itself did not demonstrate any inherent bioactivity for a period up to 28 days. The lack of bioactivity found in PET could be justified by the fact that the sponge inorganic skeleton, which is the part that would render bioactivity is not be accessible and, therefore, no nucleation of crystals occurs. In the case of the bioceramics for bone regeneration, various *in vitro* and *in vivo* studies show that a series of interfacial reactions occur that leads to the formation of an apatite layer on the glass surface responsible for bone bonding [26, 32]. The formation of an apatite layer is governed by a complex set of steps that start on the immobilization of calcium and phosphate ions in the surface of the biomaterial forming a biologically active hydroxycarbonate apatite. This layer evolves to form different calcium phosphate phases until it generates hydroxyapatite or hydroxyapatite-like coatings with their characteristic cauliflower morphology[22, 36]. When the same studies were performed to the calcinated material, the results have also shown lack of bioactivity. It is known, however that hydroxyl surface groups (-Si-OH) can be converted in Si-O-Si during processing at high temperatures in anhydrous environments [37]. Therefore, the original presence of such chemical groups could have been destroyed during the calcination stage. These findings led to the conclusion that the bioceramics from PET do not possess intrinsic bioactivity, requiring a

chemical modification to induce it. Upon this modification, the hydroxyl groups now present on the surface may act as nucleation points for the formation of hydroxyapatite, meaning the surface bioactive. This hypothesis is in fact, in agreement with the experimental results obtained after the *in vitro* bioactivity tests performed. The presence of new crystalline structures can be observed for samples after immersion in SBF for 7 and 14 days, both for the acid and alkaline modified structures. Conversely, on the unmodified samples the development of such structures is not observed. According to the results presented, the HA obtained on the alkaline treated surfaces presents a Ca/P ratio below the stoichiometric 1.67, but an increase of the ratio with time of immersion was observed. In case of samples treated with HCl the Ca/P ratio of 1.67 was obtained for immersion after 14 days. In terms of morphology, the crystals present the typical cauliflower-like shape characteristic of hydroxyapatite except for the KOH 7 days samples. As can be observed from **Figure 4**, the morphology is clearly different from the others and the EDS analysis revealed the presence of Mg in higher amounts in the crystal composition. These non-stable crystals, where other cations are present in the apatite lattice, can affect the stoichiometry of the developed apatite which will reflect in the Ca/P ratio. The Mg^{2+} will compete with Ca^{2+} for the same positions and, therefore, if the amount of phosphorus is maintained, a decrease in the ratio Ca/P is expected, this occurrence is in agreement with our results, as presented in **Table 2**. These substitutions in the apatite structure modify the crystal lattice parameters and change the solubility and bioactivity properties of the material[23, 24]. Similar results were obtained for the samples modified with the 3 hours modification procedures. Nonetheless, after 14 days of immersion these metastable crystals originate stoichiometric HA.

The results of FTIR and XRD analysis confirm the ability of the modified 3D bioceramic structure obtained from PET to act as nucleating points for the growth calcium-phosphate crystals and the success of surfaces treatments to induce bioactivity. The intermediate crystals, confirmed by XRD, formed during apatite precipitation process are unstable and will eventually lead to the formation of the stoichiometric hydroxyapatite layer on the surface of the ceramic. Comparing the results obtained for the two treatments, the same crystallographic planes were observed, demonstrating that both the alkali and acid surface modification treatments have induced the precipitation of the same apatite crystals, thus rendering the surface bioactive.

An important feature of the materials is their *in vitro* biological performance. The 3D bioceramic structure, in a biological environment, must be adequate for cell attachment, proliferation, tissue growth.

The results demonstrate an increase of cell proliferation for the surface treated samples, after 3 days in culture. The highest values for cell proliferation were obtained after 7 and 14 days of culture for HCl treated samples, while for the KOH samples have a decrease of values. The results confirm that the samples treated with HCl, which have been the ones that demonstrated to be the most bioactive, are the ones that induce the activity of ALP enzyme and consequently leading to higher mineralization. **The acidic treatment of the 3D bioceramics structures have showed to have a positive effect on the cell proliferation. This results are supported by the bioactivity assay observing a higher crystal nucleation in the samples treated by acidic conditions, wich suggest a good bioactive surface with the presence of hydroxyl groups. According to *Feng and co-works*[38], more surface hydroxyl groups resulted in greater numbers of adhered osteoblasts and higher cell activity, which support the higher metabolic activity and alkaline phosphatase activity in HCl comparing with KOH treatment. The results obtained for MTS, DNA and ALP analysis, corroborate the fact suggested that HCl treatment improved the biological activity of the 3D marine-derived bioceramic structure.**

7. CONCLUSIONS

In this study, a 3D bioceramic structure was obtained after calcination of the marine sponge *Petrosia ficidormis*. The calcination process renders a 3D bioceramic structure free of organic compounds but deprived of bioactivity. To induce bioactivity two chemical (alkaline and acidic) treatments were successful applied without modifying the overall structure, these modifications change the surface chemistry in such a way that it was able to promote precipitation of Ca/P crystals, namely hydroxyapatite, when immersed in SBF. Comparing the two chemical treatments, the HCl modification has proved to be more efficient for the nucleation of bioactive crystals. *In vitro* studies with an osteoblastic cell line have demonstrated the potential of the structure to support cell adhesion and growth. The set of results here presented have validated that the HCl modification is more effective than the one performed with KOH,

not only in terms of improvement of the bioactivity but also in what concerns cell proliferation, cell adhesion and mineralization. Finally, this study demonstrated the potential of 3D bioceramic obtained from marine sponge to be applied in tissue engineering strategies.

ACKNOWLEDGEMENTS: Alexandre Barros is grateful for financial support of FCT through grant EXP/QEQ-EPS/0745/2012, SWIMS - Subcritical Water Isolation of compounds from Marine Sponges. The research leading to these results has received funding from the European Union Seventh Framework Programme (FP7/2007-2013) under grant agreement number REGPOT-CT2012-316331-POLARIS and under grant agreement n° KBBE-2010-266033 (project SPECIAL). Funding from the project "Novel smart and biomimetic materials for innovative regenerative medicine approaches" RL1 - ABMR - NORTE-01-0124-FEDER-000016) cofinanced by North Portugal Regional Operational Programme (ON.2 – O Novo Norte), under the National Strategic Reference Framework (NSRF) is also acknowledged.

References

(1)Frenz, J. L.; Kohl, A. C.; Kerr, R. G., Marine natural products as therapeutic agents: Part 2. Expert Opinion on Therapeutic Patents ***2004,*** *14, (1), 17-33.*

(2)Blunt, J. W.; Copp, B. R.; Hu, W.-P.; Munro, M. H. G.; Northcote, P. T.; Prinsep, M. R., Marine natural products. Natural Product Reports ***2007,*** *24, (1), 31-86.*

(3)Blunt, J. W.; Copp, B. R.; Hu, W.-P.; Munro, M. H. G.; Northcote, P. T.; Prinsep, M. R., Marine natural products. Natural Product Reports ***2009,*** *26, (2), 170-244.*

(4)van Soest RWM, B.-E. N., Hooper JNA, Rützler K, de Voogd NJ, Alvarez B, Hajdu E, Pisera AB, Vacelet J, Manconi R, Schoenberg C, Janussen D, Tabachnick KR, Klautau M, In ed.; World Porifera database. Available online at http://www.marinespecies.org/porifera, 2008.

(5)Proksch, P.; Edrada, R.; Ebel, R., Drugs from the seas – current status and microbiological implications. Appl Microbiol Biotechnol ***2002,*** *59, (2-3), 125-134.*

(6)Kim, S. K., Marine Biomaterials: Characterization, Isolation and Applications. ed.; Taylor & Francis: 2013.

(7)Alexandre A. Barros , I. M. A., Tiago H. Silva , João F. Mano , Ana Rita C. Duarte , Rui L. Reis, Marine Sponges – a new source of bioactive ceramics for Tissue engineering and regenerative medicine applications. Journal of the American Ceramic Society ***2014****.*

(8)Cunningham, E.; Dunne, N.; Walker, G.; Maggs, C.; Wilcox, R.; Buchanan, F., Hydroxyapatite bone substitutes developed via replication of natural marine sponges. Journal of Materials Science-Materials in Medicine ***2010,*** *21, (8), 2255-2261.*

(9)Kamenos, N. A.; Cusack, M.; Huthwelker, T.; Lagarde, P.; Scheibling, R. E., Mg-lattice associations in red coralline algae. Geochimica et Cosmochimica Acta ***2009,*** *73, (7), 1901-1907.*

(10) Elsinger, E. C.; Leal, L., Coralline hydroxyapatite bone graft substitutes. The Journal of Foot and Ankle Surgery ***1996,*** *35, (5), 396-399.*

(11) Walsh, P. J.; Walker, G. M.; Maggs, C. A.; Buchanan, F. J., Thermal preparation of highly porous calcium phosphate bone filler derived from marine algae. Journal of Materials Science: Materials in Medicine ***2010,*** *21, (8), 2281-2286.*

(12) Schröder, H.; Brandt, D.; Schloßmacher, U.; Wang, X.; Tahir, M.; Tremel, W.; Belikov, S.; Müller, W. G., Enzymatic production of biosilica glass using enzymes from sponges: basic aspects and application in nanobiotechnology (material sciences and medicine). Naturwissenschaften ***2007,*** *94, (5), 339-359.*

(13) Schröder, H. C.; Boreiko, O.; Krasko, A.; Reiber, A.; Schwertner, H.; Müller, W. E. G., Mineralization of SaOS-2 cells on enzymatically (silicatein) modified bioactive osteoblast-stimulating surfaces. Journal of Biomedical Materials Research Part B: Applied Biomaterials ***2005,*** *75B, (2), 387-392.*

(14) Kim, S. K.; Dewapriya, P., Chapter 8 - Bioactive Compounds from Marine Sponges and Their Symbiotic Microbes: A Potential Source of Nutraceuticals. In Advances in Food and Nutrition Research, Se-Kwon, K., Ed. Academic Press: 2012; Vol. Volume 65, pp 137-151.

(15) Bavestrello, G.; Benatti, U.; Calcinai, B.; Cattaneo-Vietti, R.; Cerrano, C.; Favre, A.; Giovine, M.; Lanza, S.; Pronzato, R.; Sara, M., Body Polarity and Mineral Selectivity in the Demosponge Chondrosia reniformis. Biological Bulletin ***1998,*** *195, (2), 120-125.*

(16) Schroder, H. C.; Wang, X.; Tremel, W.; Ushijima, H.; Muller, W. E. G., Biofabrication of biosilica-glass by living organisms. Natural Product Reports ***2008,*** *25, (3), 455-474.*

(17) Müller, W. E. G., Silicon Biomineralization: Biology, Biochemistry, Molecular Biology, Biotechnology. ed.; Springer Verlag: 2003.
(18) Müller, W. E. G.; Grachev, M. A., Biosilica in Evolution, Morphogenesis, and Nanobiotechnology: Case Study Lake Baikal. ed.; Springer: 2009.
(19) Alves, N. M.; Leonor, I. B.; Azevedo, H. S.; Reis, R. L.; Mano, J. F., Designing biomaterials based on biomineralization of bone. Journal of Materials Chemistry ***2010,*** *20, (15), 2911-2921.*
(20) Schröder, H.; Obermeier, E., A new model for Si {100} convex corner undercutting in anisotropic KOH etching. Journal of Micromechanics and Microengineering ***2000,*** *10, (2), 163.*
(21) Agnihotri, S.; Mukherji, S.; Mukherji, S., Immobilized silver nanoparticles enhance contact killing and show highest efficacy: elucidation of the mechanism of bactericidal action of silver. Nanoscale ***2013,*** *5, (16), 7328-7340.*
(22) Kokubo, T.; Takadama, H., How useful is SBF in predicting in vivo bone bioactivity? Biomaterials ***2006,*** *27, (15), 2907-2915.*
(23) Ducheyne, P.; Healy, K. E.; Hutmacher, D. E.; Kirkpatrick, C. J., Comprehensive Biomaterials. ed.; Elsevier Science & Technology Books: 2011.
(24) Low, K. L.; Tan, S. H.; Zein, S. H. S.; Roether, J. A.; Mourino, V.; Boccaccini, A. R., Calcium phosphate-based composites as injectable bone substitute materials. J Biomed Mater Res B ***2010,*** *94B, (1), 273-286.*
(25) Silva, T. H.; Alves, A.; Ferreira, B. M.; Oliveira, J. M.; Reys, L. L.; Ferreira, R. J. F.; Sousa, R. A.; Silva, S. S.; Mano, J. F.; Reis, R. L., Materials of marine origin: a review on polymers and ceramics of biomedical interest. International Materials Reviews ***2012,*** *57, (5), 276-306.*
(26) Tancred, D. C.; McCormack, B. A. O.; Carr, A. J., A synthetic bone implant macroscopically identical to cancellous bone. Biomaterials ***1998,*** *19, (24), 2303-2311.*
(27) Hutmacher, D. W.; Schantz, T.; Zein, I.; Ng, K. W.; Teoh, S. H.; Tan, K. C., Mechanical properties and cell cultural response of polycaprolactone scaffolds designed and fabricated via fused deposition modeling. Journal of Biomedical Materials Research ***2001,*** *55, (2), 203-216.*
(28) Karageorgiou, V.; Kaplan, D., Porosity of 3D biomaterial scaffolds and osteogenesis. Biomaterials ***2005,*** *26, (27), 5474-5491.*
(29) An, Y. H.; Draughn, R. A., Mechanical Testing of Bone and the Bone-Implant Interface. ed.; Taylor & Francis: 1999.
(30) Hench, L. L.; Wilson, J., An Introduction to Bioceramics. ed.; World Scientific: 1993.
(31) Oliveira, A.; Mano, J.; Reis, R., Nature-inspired calcium phosphate coatings: present status and novel advances in the science of mimicry. Current Opinion in Solid State and Materials Science ***2003,*** *7, (4), 309-318.*
(32) Dorozhkin, S. V., Bioceramics of calcium orthophosphates. Biomaterials ***2010,*** *31, (7), 1465-1485.*
(33) Huang, Y.-C.; Hsiao, P.-C.; Chai, H.-J., Hydroxyapatite extracted from fish scale: Effects on MG63 osteoblast-like cells. Ceramics International ***2011,*** *37, (6), 1825-1831.*
(34) Oliveira, J. M.; Grech, J. M. R.; Leonor, I. B.; Mano, J. F.; Reis, R. L., Calcium-phosphate derived from mineralized algae for bone tissue engineering applications. Materials Letters ***2007,*** *61, (16), 3495-3499.*
(35) Luz, G. M.; Mano, J. F., Mineralized structures in nature: Examples and inspirations for the design of new composite materials and biomaterials. Composites Science and Technology ***2010,*** *70, (13), 1777-1788.*

(36) Benhayoune, H.; Charlier, D.; Jallot, E.; Laquerriere, P.; Balossier, G.; Bonhomme, P., Evaluation of the Ca/P concentration ratio in hydroxyapatite by STEM-EDXS: influence of the electron irradiation dose and temperature processing. J Phys D Appl Phys ***2001,*** *34, (1), 141-147.*

(37) Zhuravlev, L. T., The surface chemistry of amorphous silica. Zhuravlev model. Colloids and Surfaces A: Physicochemical and Engineering Aspects ***2000,*** *173, (1–3), 1-38.*

(38) Feng, B.; Weng, J.; Yang, B. C.; Qu, S. X.; Zhang, X. D., Characterization of surface oxide films on titanium and adhesion of osteoblast. Biomaterials ***2003,*** *24, (25), 4663-70.*

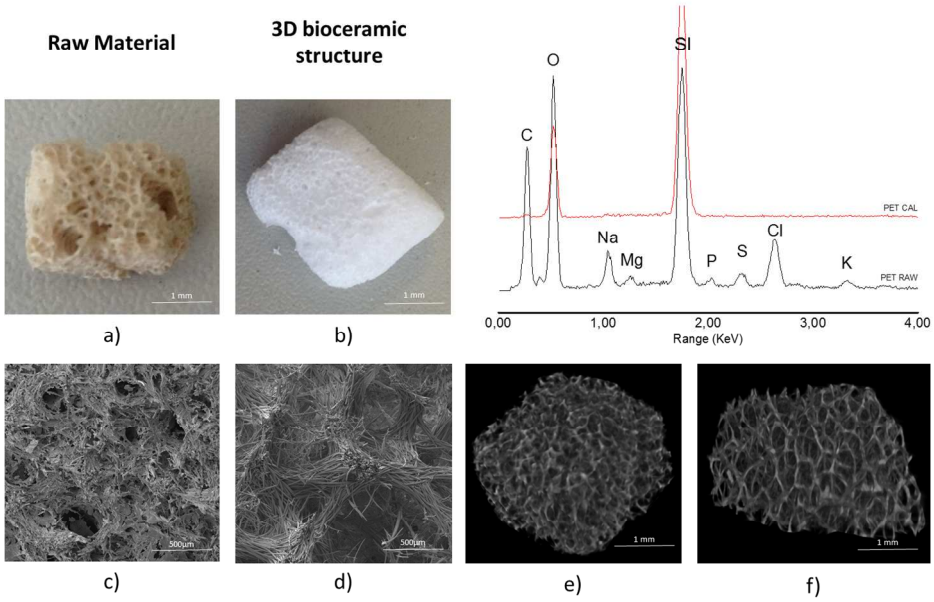

Figure 1. Morphological characterization of Petrosia ficidormis before and after calcination: (a,b) magnifying lens 1x (c,d) SEM micrographs (e, f) 3D micro-CT reconstruction images. EDS spectra chemical characterization of the structures (top right).
436x286mm (300 x 300 DPI)

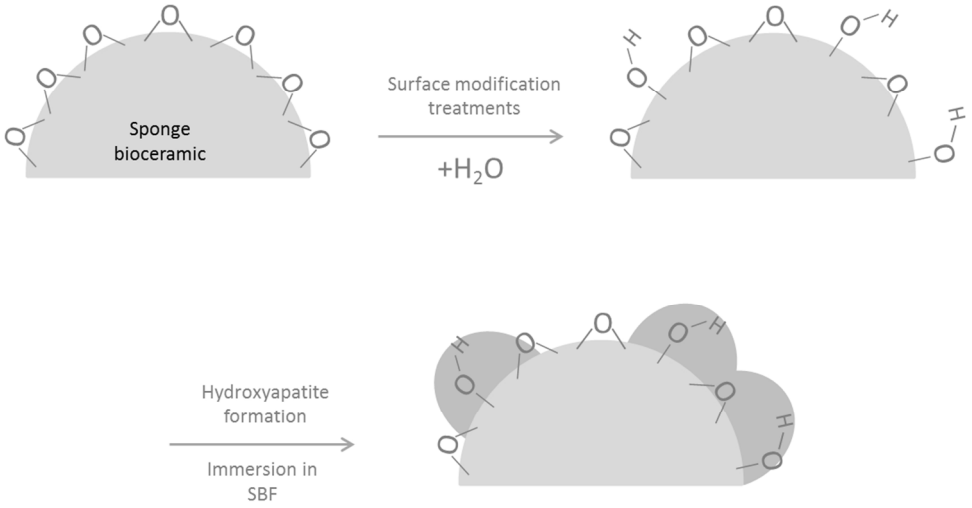

Figure 2 - Schematic representation of the surface modification of the sponge bioceramics surface modification and apatite formation.
321x171mm (300 x 300 DPI)

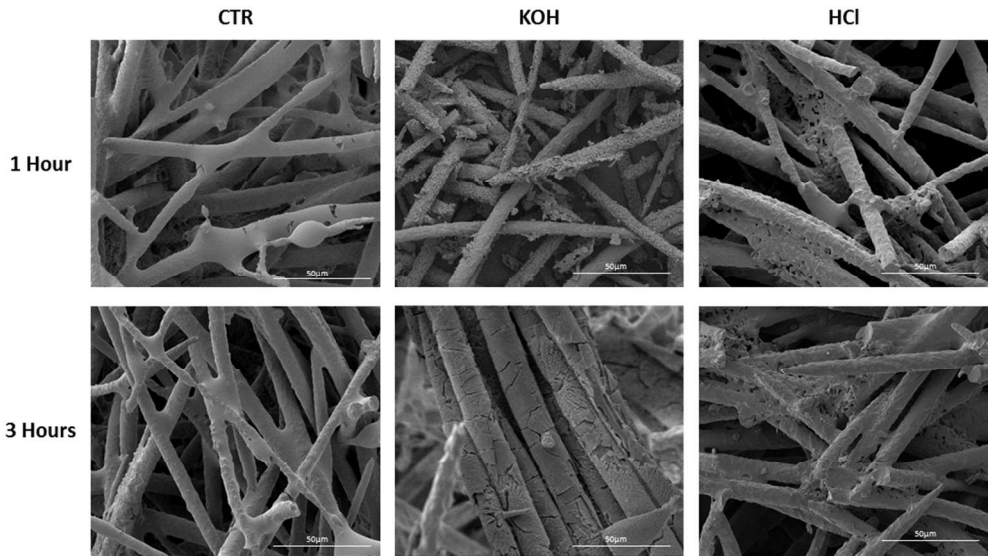

Figure 3. SEM images after treatment in KOH and HCl during 1hour and 3 hours of reactions. 3D bioceramic without treatment was used as a control.
293x163mm (300 x 300 DPI)

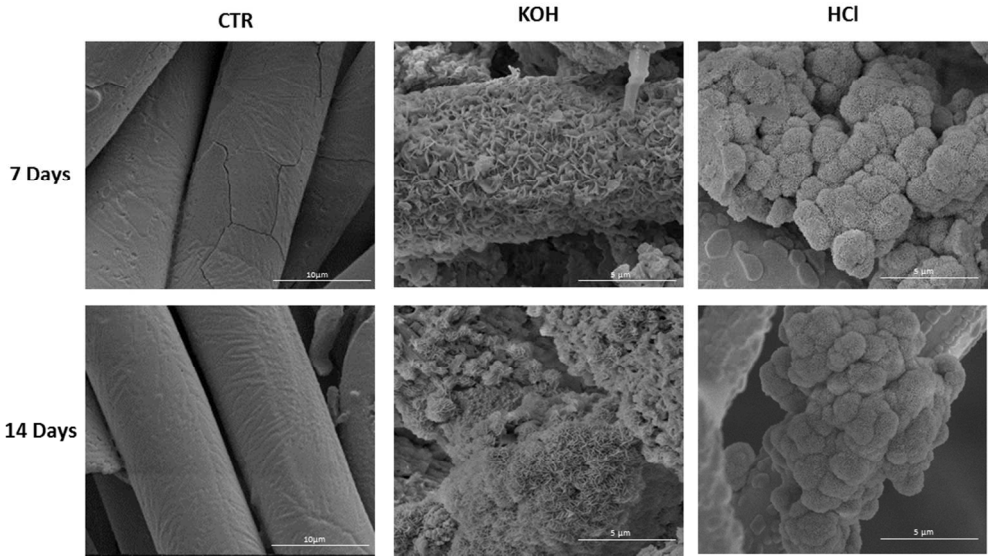

Figure 4. SEM images of bioactivity studies after chemical treatments (reaction time 1 hour).
293x165mm (300 x 300 DPI)

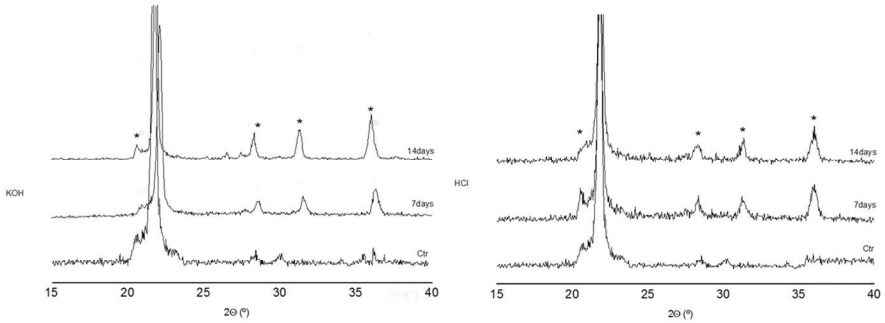

Figure 5. X-ray powder patterns of the 3D bioceramic structures of KOH and HCl treatments (1 hour reaction), before and after immersion in SBF solution (7 and 14 days).
376x150mm (300 x 300 DPI)

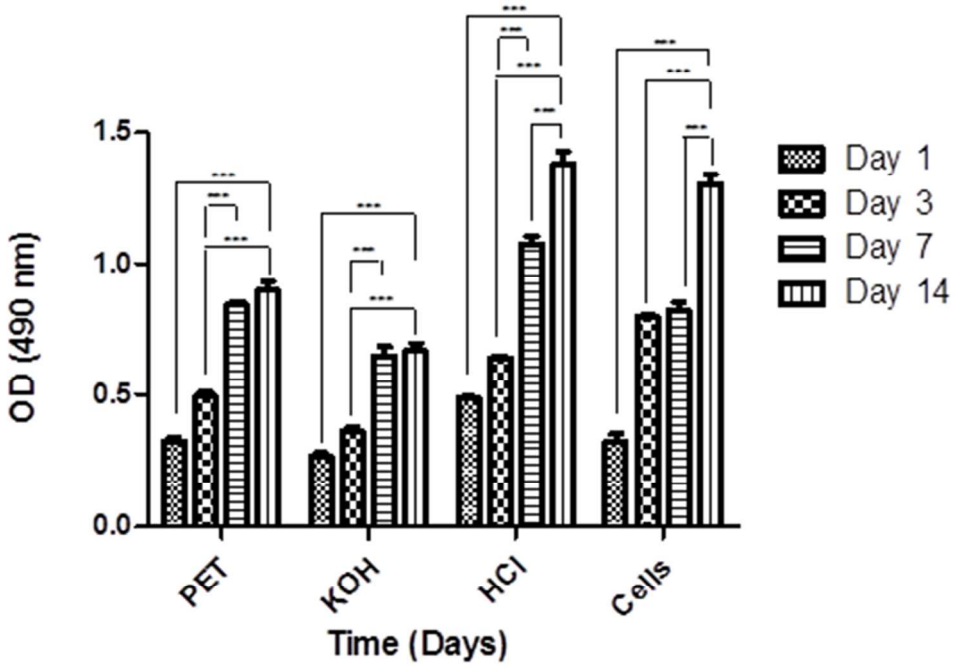

Figure 6. Metabolic activity of SaOS-2 cultured for 1, 3, 7 and 14 days with 3D Bioceramics structures of KOH and HCl treatments (1hour reaction). Metabolic activity was extrapolated from the optical density resultant from the MTS reduction by the cells. Control (CTR) corresponds to cells cultured on tissue culture polystyrene.
127x91mm (300 x 300 DPI)

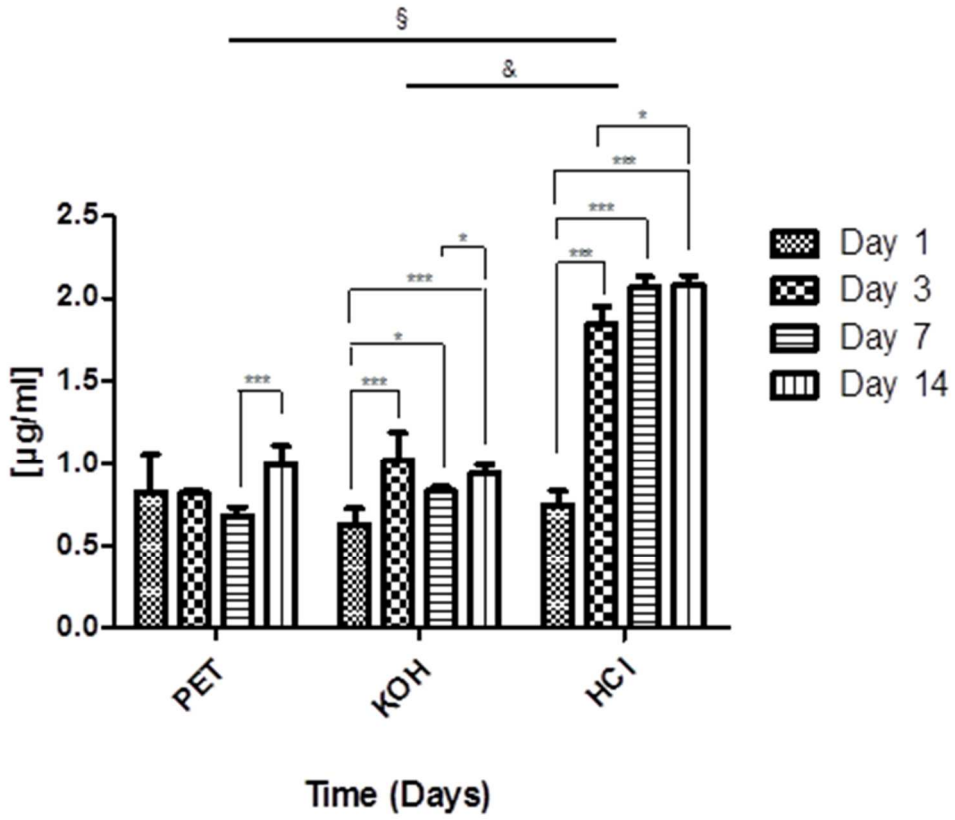

Figure 7. Double stranded DNA (dsDNA) content of SaOS-2 cells cultured for 1,3,7 and 14 days on 3D Bioceramics structures of KOH and HCl treatments(1 hour reaction). The differences are significant (*, & and § $p < 0.05$; *** $p < 0.001$).
122x107mm (300 x 300 DPI)

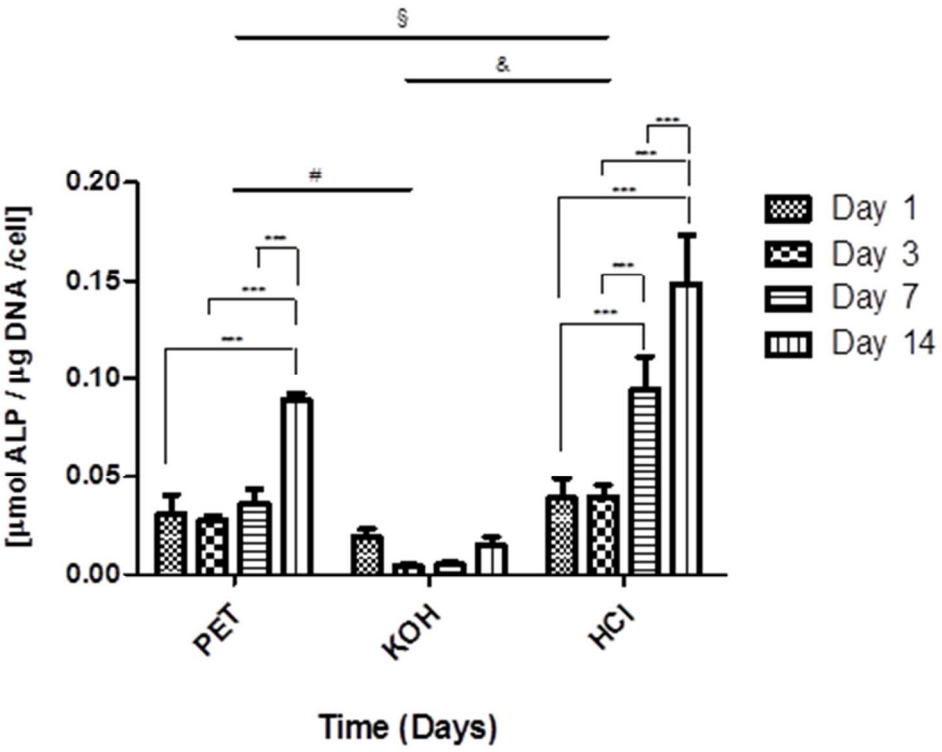

Figure 8. Quantification of the amount of hydrolysed p-nitrophenol phosphate that correlates with alkaline phosphatase (ALP) activity in SaOS-2 Cells after 1,3, 7 and 14 days of culture on 3D Bioceramics structures of KOH and HCl treatments (1hour reaction). The differences are significant (#, & and § $p < 0.05$; *** $p < 0.001$).
128x102mm (300 x 300 DPI)

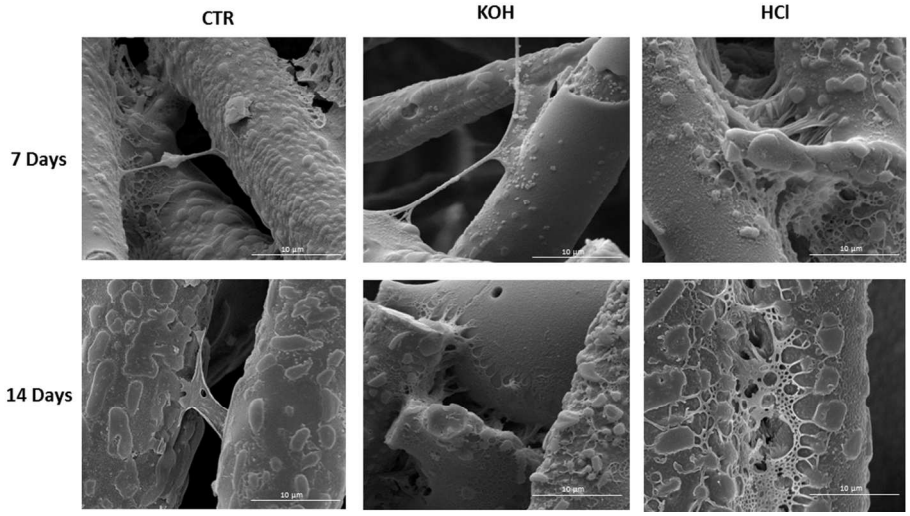

Figure 9. SEM images of SaOS-2 cells adhesion after 7 and 14 days of culture on 3D Bioceramics structures of KOH and HCl treatments (1 hour reaction).
320x166mm (300 x 300 DPI)

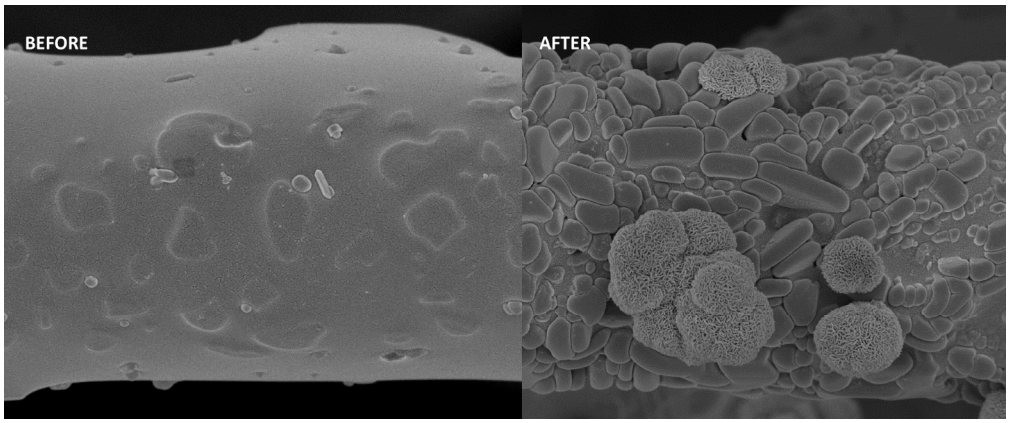

TOC Graphic - Marine sponge bioceramics have been modified, through simple chemical procedures and rendered bioactive materials, as shown by the induced formation of hydroxyapatite. These surfaces are suitable to support for cell growth engaging their use in bone tissue applications
329x136mm (299 x 299 DPI)